Difference in the bed load transport of graded and uniform sediments during floods: An experimental investigation

Khabat Khosravi, Amir H. N. Chegini, Andrew D. Binns, Prasad Daggupati and Luca Mao

ABSTRACT

The objective of this study was to experimentally evaluate the difference in the transport of uniform (5.17, 10.35, 14, 20.7 mm) and graded sediment (mixture of these rounded particles with equal weight proportions) under different unsteady flow hydrographs in a 12 m long, 0.5 m wide and deep glass-walled flume. There was a lag time between fractions and uniform particles, such that peaks of coarser and finer fraction particles occurred before and after the peak of uniform sediment with the same size, respectively. Comparison between uniform particles and fractions in graded sediment showed that the sediment transport rate of fine and coarse fractions was lower and higher than their counterpart uniform particles, respectively. Overall, the uniform particles demonstrated a clockwise hysteresis loop and graded sediment had a counterclockwise hysteresis loop. The mobility of coarser fractions increased during the rising limb of hydrograph, whereas the mobility of finer fractions increased during the falling limb. In general, the mobility of coarse fractions increased and that of fine fractions reduced. Result of transported sediment showed that average particle size collected in traps (D_{b50}) was coarser than bed material (D_{s50}) on both limbs. The relative transport ratio for uniform and graded sediment is higher and lower than 1, respectively.

Key words | bed load, experimental investigation, graded sediment, hysteresis loop, mobility, unsteady flow hydrograph

Khabat Khosravi
Andrew D. Binns
Prasad Daggupati
School of Engineering,
University of Guelph,
Guelph,
Canada

Amir H. N. Chegini (corresponding author)
School of the Built Environment,
Heriot-Watt University,
Edinburgh,
UK
E-mail: *ahnchegini@yahoo.co.uk*

Luca Mao
School of Geography,
University of Lincoln,
Lincoln,
UK

INTRODUCTION

Sediment transport dynamics during floods determine the morphology of rivers (Church 2006), with relevant consequences for public health and safety, water management, fluvial ecology, and sustainable development of riverine areas (Chien & Wan 1999; Raven *et al.* 2010). Depending on the flow strength and the size of sediments, the grains can be transported as either suspended or bed load (Li *et al.* 2016), with bed load transport being the primary driver for river morphodynamics (Church 2006).

Sediment transport has been studied extensively under steady-state conditions (i.e., with constant discharge) (Barati *et al.* 2014, 2018; Barati & Salehi Neyshabouri 2019). However, sediment transport and river processes during flood events are arguably very different from those that occur during these steady flows (e.g., Chien *et al.* 1987; Rowinski & Czernuszenko 1998; De Sutter *et al.* 2001). Bombar *et al.* (2011) argued that in unsteady flow, the turbulence intensity along the flow path and the vertical axis was greater, producing a greater lift force acting on bed and suspended sediments, and therefore traditional sediment transport formulae underestimate the true sediment load (Song & Graf 1997). Thus, it is not surprising that sediment

doi: 10.2166/nh.2019.078

transport formulae developed under steady uniform flow conditions perform unsatisfactorily for engineering projects.

Sediment transport during flood events often exhibits hysteresis because of the lag between the peak of the flow and sediment discharge (Reid *et al.* 1985). Several examples of hysteresis have been reported. Generally, there are five types of hysteresis loops, including clockwise, counterclockwise, eight-shaped, irregular (complex), and linear (Lenzi & Marchi 2000; Keesstra *et al.* 2018, 2019). Clockwise loops are the most common ones observed in the field (Seeger *et al.* 2004), especially for suspended sediment transport when the peak of sediment transport rate takes place before the discharge peak (Klein 1984; Soler *et al.* 2008; Eder *et al.* 2010). When the peak of sediment transport rate takes place after the discharge peak, a counterclockwise pattern is observed. This loop has been related to the breakdown of the armor layer (Kuhnle 1992), delay of the sediment supply (Habersack *et al.* 2001), passage of bed forms (Bell & Sutherland 1983), and consolidation of bed materials during flood events (Reid *et al.* 1985). When the sediment source is far away from the river, eight-shape loops will be constructed. In this case, the second loop appears in the recession limb of the hydrograph just after either a clockwise or counterclockwise loop (Zabaleta *et al.* 2007). Complex loop is constructed when there is a double-peaked hydrograph.

In alluvial rivers, hydrographs and graded sediment transport are intrinsically linked (Phillips & Sutherland 1990; Huygens *et al.* 2000; Berta & Bianco 2010). Studies on bed load transport during floods began in the 1980s (Wang *et al.* 2015), but direct observation of bed load during high flow is notoriously challenging and dangerous, thus recent studies tend to focus on flume experiments (Graf & Qu 2004; Mao 2012). Unsteady flow is usually investigated by modeling the temporal variability of flow rate during a hydrograph generating triangular and trapezoidal hydrographs (e.g., Lee *et al.* 2004; Bombar *et al.* 2011). Alternatively, hydrographs are often modeled by consecutive steps of steady flows with short intervals, named quasi-steady flows (i.e., stepped hydrographs) (Parker *et al.* 2007; Piedra 2010; Mao 2012). This type of simulation tends to lead to errors in the calculation of sediment transport (Nouh 1988), and the best alternative is to simulate continuous unsteady flow.

Tsujimoto (1989) discussed two mechanisms associated with sediment transport during floods, with the first mechanism involving the direct impact of unsteady flow and the second involving an indirect impact of relaxation processes, which is a slow response of sediment transport to the flow condition. Investigations on boundary layers in unsteady turbulent flow showed that unsteadiness effects were often limited to a thin layer close to the wall, while the outer areas were not strongly affected (Karimaee Tabarestani & Zarrati 2014). Hence, the data of outer areas may not correctly reflect the unsteadiness effects on the most effective internal variable parameters, namely, bed shear velocity (Pathirana *et al.* 2006). Consequently, the structure of unsteady flow field may differ from that of steady flow field.

Lee *et al.* (2004) investigated uniform bed load transport under unsteady flow in a laboratory and found a lag time (approximately 6–15% of the hydrograph duration) between the values of maximum flow discharge and maximum sediment discharge as a result of particle size. Their result showed that bed load sediment transport under unsteady conditions was higher than the values predicted under steady conditions and the maximum bed sediment discharge was also greater than the predicted value. A certain interval between the peak of flow discharge and peak of sediment discharge was also observed by Wang (1994), and was named 'bed inertia lag'. Wang *et al.* (2015) examined graded sediment transport (as unimodal and bimodal) influenced by various hydrographs of unsteady flow on a slope of 0.0083 m m^{-1} and found that the transport of the major coarse and the fine fraction occurred during the rising and falling limbs of hydrograph, respectively. They also stated that the peak of coarse sediment discharge occurred close to or a little earlier than the discharge peak, and it occurred after the discharge peak for fine particles. Hassan *et al.* (2006) used a graded and relatively coarse mixture (0.18 to 45 mm) to simulate hydrographs of different duration, magnitude, and shape in order to examine the effect of hydrographs on sediment transport and on the development of armoring. In their experiments, Hassan *et al.* (2006) did not feed sediments from the upstream end of the flume, and thus simulated hydrographs under sediment starvation conditions forced the creation of static armor. Mao (2012) evaluated the effect of three types of stepped hydrographs on fractional

bed load sediment transport in graded sediments (20% gravel and 80% sand), constant slope of 0.01 m m^{-1}, and sediment recirculation conditions. His results showed that in all three models, sediment discharge was higher during the rising limb than during the recession limb. He also reported that the grain size of the armor bed remained invariant during the experiments, and that sediment transport showed clockwise hysteresis. Guney *et al.* (2013) investigated the effect of coarse surface establishment on the sediment transport rate under an unsteady flow hydrograph for a bimodal sediment mixture. Their result showed that there is a strong linear relationship between armor ratio and total sediment transport yield, with a correlation coefficient of 0.99. Also, they revealed that, at first, clockwise hysteresis appeared but after armor development the hysteresis switched to counterclockwise. Li *et al.* (2018) have studied the effect of sand on gravel (and vice versa) using both unsteady and volume equivalent steady flow and revealed that unsteady flows can cause greater transport of sediment than steady flows, sand promotes the transport of gravel, and gravel reduces the transport of sand. Similarly, Mrokowska & Rowinski (2019) studied the effect of several triangular, trapezoidal, and step-wise hydrographs on different sand–gravel, silt–gravel, silt–sand mixtures, and tri-modal sand–gravel mixtures. Some researchers introduced suitable dimensionless parameters to determine the relationship between unsteadiness of flow and sediment transport in the flow hydrograph (e.g., Graf & Suszka 1985; Yen & Lee 1995), but, although important, this issue has attracted little attention thus far. In particular, to our knowledge, no studies have studied the response of graded fraction and their same-sized uniform counterpart to unsteady flow, and studied how the difference in mobility varies with bed slope and particle diameter.

This paper aims to address this research gap by reporting on 15 flume experiments designed using different bed material and unsteady flow hydrographs to study the difference in transport of graded and uniform bed sediment, and its temporal variation, in response to unsteady flow conditions. As well as investigating how this difference varies with bed slope and particle diameter, this paper also explores the relationship between the Einstein bed load parameter and Shield stress for unsteady flow. Also, differences between hysteresis of uniform and graded bed sediment are addressed.

MATERIALS AND METHODS

Flume set-up

A 12 m long, 0.5 m wide, tilting flume was used in this study (Figure 1). The flume walls were made of transparent glass. Experiments were done with slopes ranging from 0.005 to 0.035 m m^{-1}. Runs were performed using four homogeneous grain sizes (5.17, 10.35, 14, and 20.7 mm) and a graded mixture made up using the four classes with equal weight ratio (Table 1). Sediment beds were created by screeding the sediment to a depth of ~5–6 $D_{50,}$ and remixed and screeded for subsequent runs. The upstream and downstream parts of the flume (each 2 m long) were non-movable. For the 2 m fixed upstream section, the 1 m upstream end was covered by coarse sediments (20.7 mm) and the 1 m

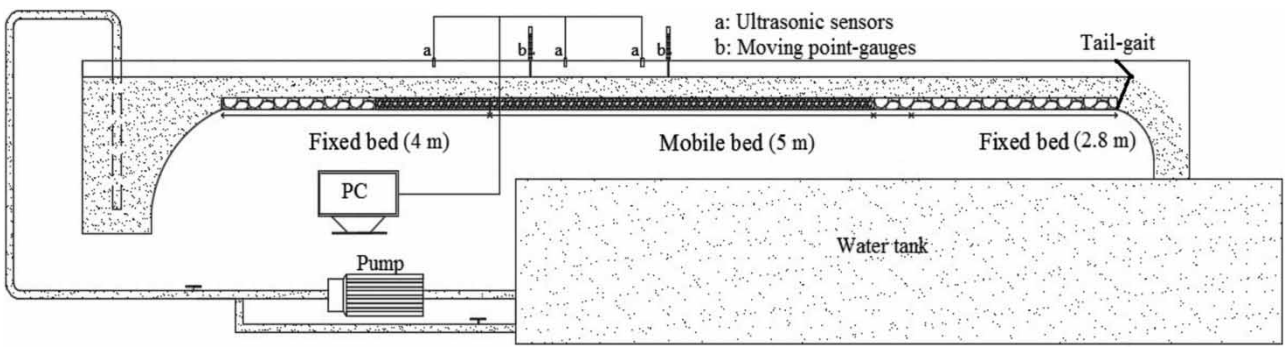

Figure 1 | Schematic view of experimental flume and its equipment in this study.

Table 1 | Physical properties of bed sediments used in the study

Sediment	D_{50} (mm)	σ_g	Density, (kg/m^3)	Porosity (−)
Fine gravel	5.17	–	2,391	0.4
Medium gravel lower	10.35	–	2,375	0.4
Higher medium gravel	14	–	2,900	0.45
Coarse gravel	20.7	–	2,552	0.43
Graded (mixture)	12.5	1.8	2,567	0.37

The geometric standard deviation was calculated as $\sigma_g = (D_{84}/D_{16})^{0.5}$.

fixed downstream section was covered by the same sediment as used in the mobile sections. The 2 m long fixed section at the downstream end of the flume was covered by 20.7 mm sediments. This arrangement gave an erodible bed section with a length of 8 m. For water supply, a closed-circuit flow was used in the flume, using a pump capable of producing a maximum discharge up to 100 L s^{-1}. The water depth in the flume was measured by two point gauges (b_1 and b_2; Figure 1) and three ultrasonic sensors (a_1, a_2, and a_3) recording the water level with a frequency of 25 Hz. Sensor a_1 was placed over the fixed bed, whereas sensors a_2 and a_3 were placed over the mobile bed portion of the flume. The distances between the first and second sensors and between the second and third ones were 2 m and 1 m, respectively (Figure 1).

Experimental procedure for simulating hydrographs

Experiments were designed to simulate hydrographs using unsteady flow conditions. At the beginning of each run, the downstream tailgate was raised and then the pump was turned on at the lowest flow rate to ensure the minimum disturbance to the bed during the time required for the initial wetting stages. Then, the desired base flow ($Q_0 = 3$ L s^{-1}; at which point no sediment moved at any slope) was attained to perform uniform steady flow conditions for 1 h to produce a water-worked surface and to ensure that all experiments were performed with the same initial bed condition. In this stage, the tailgate was lowered to have a uniform steady flow as well as reduce the backwater effect (Wang *et al.* 2015). The flow depth to establish steady flow was checked by point gauge and ultrasonic sensors at the upstream and downstream mobile bed sections. Each run started ($t = 0$) when the flow began to increase. Hydrographs were created by programming the opening and closing of the valves in a continuous process over time, with flow velocity, flow depth, and discharge measured every minute. Bed load sediment transport rate was measured using a bed load trap (0.3 m wide and 0.5 m long) located at the downstream end of the flume. Samples of transported sediment were taken during the passage of the hydrograph, for a duration ranging from 1 to 20 min depending on the sediment transport intensity (it is noted that the frequency of sampling was high enough particularly before and after peak flow to resolve the peak flow and sediment lag). The level of variability in peak transport rates near the peak flow was considered for calculation of the lag time between peak of flow and sediment transport. The collected sediment samples were dried, sieved (for graded sediment), and weighed in order to obtain the total and fractional transport rate. As in Hassan *et al.* (2006), Wang *et al.* (2015), and Li *et al.* (2018), no sediments were fed from the upstream end of the flume during the experiments. This zero-feeding condition, which is responsible for clean water scouring, is a reasonable simplification during short-term periods for rivers in humid environments (see Hassan *et al.* 2006; Wang *et al.* 2015; Li *et al.* 2018) and is similar to conditions downstream of dams.

The simulated unsteady flow hydrograph

The runs simulated an asymmetric hydrograph with a peak of 70 L s^{-1}, a total volume, excluding base flow, equal to 165 m^3, and a normal duration of 5,220 s. In some cases, especially for graded sediment with higher slopes, due to high sediment transport and extensive bed morphological changes, this duration was not possible and a shorter duration was performed (e.g., 2,400 s). The designed hydrograph is not exactly scaled to a specific prototype, but the overall shape (e.g., a longer rising limb) reflects the shape of the last five flood events in Sefid-Rud River (second largest river in Iran). The main aim for the recession limb not reaching base flow again is: (1) there was no sediment transport observed for water depth less than 7 cm for the recession limb; and (2) the shape of these flood hydrographs in Sefid-Rud River is a multiple peak hydrograph and the raising limb of the next hydrograph starts before reaching base flow. Thus our recession limb did not reach base

flow according to the general shape of these single peak hydrographs.

The hydrograph can be scaled by dimensionless terms for discharge (Q^*) and time (t^*):

$$Q^* = Q/Q_0 = Q/V_0 h_0 B \tag{1}$$

where Q is the discharge, Q_0 is the discharge at base flow, V_0 is the mean flow velocity at base flow, h_0 is the flow height at base flow, and B is the width of the flume, and

$$t^* = t/T \tag{2}$$

where t is the measurement time, and T is the total duration of the hydrograph calculated as the sum of the duration of the rising and the recession limbs, T_r and T_f, respectively. The hydrographs were characterized by an unsteadiness parameter Γ (see also Graf & Suszka (1985)) calculated as:

$$\Gamma = \Delta H/(V_0^* \times T) \tag{3}$$

where ΔH is the difference in flow heights between the maximum discharge and the base flow, and V_0^* is the bed shear velocity at base flow.

As done in previous studies dealing with unsteady flow (e.g., Yen & Lee 1995; Lee *et al.* 2004; Bombar *et al.* 2011; Wang *et al.* 2015), the magnitude of the hydrograph W_k was calculated as:

$$W_k = \frac{V_0^{*2} V_h}{g h_0^3 B} \tag{4}$$

Parameters Γ and W_k are independent of each other and it is possible that different hydrographs feature the same Γ but different values of W_k, or vice versa. Bombar *et al.* (2011), Lee *et al.* (2004), and Wang *et al.* (2015) have shown that unsteady flow properties, such as the unsteadiness parameter (Γ), total volume of hydrograph (V_h), and hydrograph shape (η) (calculated as T_r/T_f ratio), have a significant impact on bed load sediment transport. The first two properties were considered in this study but due to the fact that hydrograph shape did not change significantly in the present study and since all of them have a similar shape, hydrograph shape was not considered as an effective factor. In total, 15 tests were conducted using different slopes and sediment sizes (Table 2).

Bed load sediment transport

The cumulative sediment flux during each run was calculated as a normalized sediment transport yield (see Bombar *et al.* 2011), W_t^* as follows:

$$W_t^* = W_t/(\rho_s b D_{s50}^2) \tag{5}$$

where W_t is the total sediment transport yield in kg, ρ_s is the density of bed material, b is the width of the sediment trap (m), and D_{s50} is the average particle size of the bed material (m). For the graded mixture, fractional sediment transport yield was calculated for each grain size.

The dimensionless Einstein bed load parameter was used to compare between various transported sediments and is expressed as (Pender *et al.* 2007):

$$q_b^* = \frac{q_b}{\rho_s \sqrt{(s-1) g D_{b50}^3}} \quad q_{bi}^* = \frac{q_{bi}}{f_i \rho_s \sqrt{(s-1) g D_i^3}} \tag{6}$$

where q_b and q_{bi} are the bed load sediment transport rates (kg m^{-1} s^{-1}) for total or uniform particles and fractional transport rate, respectively, s is the relative density for bed sediment which is equal to sediment density divided by water density, g is the gravitational acceleration, D_{b50} is the average size of sediment transported to trap, D_i is the uniform material diameter or fraction material diameter, and f_i is the proportion of the fraction i in the bed surface (Shvidchenko *et al.* 2001). The Shields stress τ^* was estimated as follows:

$$\tau^* = \frac{\tau}{g(\rho_s - \rho)} = \frac{R_b S}{(s-1) d_i} \tag{7}$$

where $\tau = \rho g R_b S$ is the mean bed shear stress, ρ is fluid density, R_b is the hydraulic radius of the bed, which is corrected for the effect of the wall of the flume using the method outlined in Shvidchenko & Pender (2000), and S is the bed slope. Shear velocity (V^*) was estimated as:

$$V^* = \sqrt{\frac{\tau}{\rho}} \tag{8}$$

The dimensionless parameter of V^*/ω_S was applied to determine the suspension condition, where the ω_s is the submerged particle fall velocity. It was used to determine the

Table 2 | Important variables describing experiments done during unsteady flow hydrograph

No	Running code	D, mm	S	Q_{peak} L/s	V^*, m/s	$\tau*$	Tr, s	Tf, s	ζ	Γ	W_k	W_t^*	Fr	Re	Transport rate kg m^{-1} s^{-1}
1	A	5.17	0.005	46	0.031–0.071	0.013–0.07	3,000	2,280	0.98	0.000614	2,792.8	212.8	0.67–1.1	5,555–97,297	0.0069
2	B		0.0075	42.5	0.038–0.08	0.02–0.09	2,400	1,380	1.8	0.000561	2,701.9	1,136.9	0.7–0.85	5,783–60,791	0.069
3	C		0.01	41.5	0.044–0.088	0.02–0.11	2,160	840	3.1	0.000535	2,752.7	1,622.4	0.8–0.98	6,678–61,132	0.129
4	D	10.35	0.01	59	0.044–0.1	0.013–0.073	3,000	2,220	1.68	0.000438	7,106.3	435.03	0.7–0.9	5,969–70,898	0.05
5	E		0.015	54	0.053–0.114	0.02–0.093	2,400	1,560	4.24	0.000377	7,269.2	579.6	0.8–1.1	7,311–77,643	0.19
6	F	14	0.015	69.5	0.054–0.125	0.01–0.059	3,000	2,280	10.3	0.000353	12,661.0	78.4	0.78–1.08	6,961–93,903	0.089
7	G		0.0175	65	0.058–0.129	0.012–0.064	2,700	1,740	1.7	0.000346	11,739.9	215.02	0.9–1.14	7,519–90,766	0.12
8	H		0.02	70	0.062–0.138	0.014–0.073	2,760	1,740	2.5	0.000323	14,343.4	308.5	1–1.22	8,038–97,033	0.21
9	I		0.03	51.5	0.076–0.147	0.02–0.082	2,580	780	9.6	0.000306	8,719.7	399.91	1.2–1.45	9,885–78,103	0.38
10	J	20.7	0.03	69	0.076–0.163	0.018–0.084	2,400	1,380	1.4	0.000279	17,774.1	117.2	1.1–1.39	9,239–98,992	0.13
11	K		0.0325	72	0.08–0.17	0.019–0.09	2,400	1,380	7.8	0.000268	20,041.6	118.7	1.17–1.45	9,616–103,034	0.29
12	L		0.035	63	0.082–0.168	0.021–0.089	2,100	900	5.1	0.000285	14,790.3	166.6	1.2–1.49	9,979–92,912	0.4
13	M	Graded	0.015	70	0.053–0.124	0.014–0.08	3,000	2,220	0.3	0.000358	12,717.6	40.5	0.8–1.08	7,090–95,472	0.0058
14	N		0.02	61	0.06–0.132	0.019–0.09	2,400	1,380	0.7	0.000342	10,401.1	193.8	1–1.23	8,187–84,889	0.12
15	O		0.03	42	0.07–0.0138	0.029–0.098	1,500	900	0.5	0.000275	6,422.8	254.1	1.22–1.44	10,027–61,881	0.162

dominant transport mode when designing the hydrographs. According to Bagnold (1966), when this dimensionless parameter is less than 0.25 all particles are transported as the bed load. The ω_s term was calculated as follows (Table 3):

$$\omega_S = \frac{\sqrt{2.3(\rho_s - 1)D_{50}^2 + 36\nu^2} - 6\nu}{D_{50}} \quad (9)$$

where ν is the kinematic viscosity. The V^*/ω_S was less than 0.25 for all experimental runs, and thus, all the transported particles moved as bed load.

The fractional bed load mobility was calculated using the equation proposed by Parker & Klingeman (1982):

$$\Psi i = \frac{P_i}{F_i} \quad (10)$$

where P_i and F_i represent the fractional proportions (by weight) in bed load samples collected in the traps and in the original mixture in the bed, respectively. If $\Psi i < 1$, then the transported material had a reduced mobility in comparison to the original bed composition due to the concealment of the finer fractions. If $\Psi i = 1$ then the transported and bed material were equally mobile (state of equal mobility). If $\Psi i > 1$, the transported material had enhanced mobility compared to the original bed composition due to exposure of the coarser fractions.

RESULTS

Sediment transport rate during hydrographs with different bed slope

Temporal variations of sediment transport rate (q_b, in kg m^{-1} s^{-1}) are shown in Figure 2(a)–2(d) for the runs conducted using uniform sediments and for the graded sediment, three slopes of 0.015, 0.02, and 0.03 m m^{-1} were considered (Figure 3). Generally, by increasing the bed slope, the sediment transport rate increased. By increasing the bed slope 1.4 times, the sediment transport rate increased by 5, 4.2, 4, and 3.5 times for uniform bed sediment of 5.17, 10.35, 14, and 20.7 mm, respectively. It shows that the sediment transport rate of coarser sediments increased at a lower rate compared to the finer sediments for an increase in bed slope.

Finer uniform sediments (e.g., 5.17, 10.35, and 14 mm) demonstrate a greater increasing trend in Einstein bed load parameter with increasing bed slope in comparison to the graded sediment. However, the coarse uniform bed sediment of 20.7 mm demonstrated a similar trend with that of the graded bed sediment (Figure 4).

Also the results of ratio of total weights of transported uniform sediment (kg) per graded bed sediment in a different bed slope are shown in Table 4. The results show that with a constant bed slope of 0.015 m m^{-1}, the uniform bed sediment of 10.35 mm has a higher bed sediment transport rate than graded bed sediment (25 times more). In comparison to graded bed sediment conditions, results shows that uniform bed sediment of 14 mm has a 3.1, 1.1, and 0.74 times higher ratio of total weights of transported sediment in constant bed slope of 0.015, 0.02, and 0.03 m m^{-1}, respectively. For uniform bed material of 20.7 mm, the ratio is 0.76 times in comparison to graded bed sediments for the conditions with a bed slope of 0.03 mm^{-1}. Results of this table show that: (1) finer uniform bed sediment has a higher sediment transport rate than graded bed sediment, but the opposite trend is observed for coarser sediment; (2) with a constant bed slope of 0.015 m m^{-1}, the coarser the uniform sediment from 10.35 mm to 14 mm, the lower the difference in sediment transport rate between uniform and graded sediment; and (3) the higher the bed slope, the lower the difference in sediment transport rate between uniform and graded sediment (as with increasing the bed slope from 0.015 to 0.03 m m^{-1} the ratio of uniform bed sediment of 14 mm per graded decreased from 3.1 to 0.74 times, respectively).

One considerable difference between uniform and graded bed sediment is that the peak transport rate of all bed sediment occurred before the hydrograph peak, but the peak of graded bed sediment transport occurred after the hydrograph peak. At this slope and at a slope of

Table 3 | Determination of transport mode at different flume slopes

S	D (mm)	Y_{max} (cm)	V* (m/s)	ω_S (m/s)	$V*/\omega_S$
0.015	10.35	11	0.114	73	0.0015
0.03	14	8	0.147	81	0.0018
0.01	5.17	9	0.088	74	0.0011
0.035	20.7	9	0.168	76	0.0022

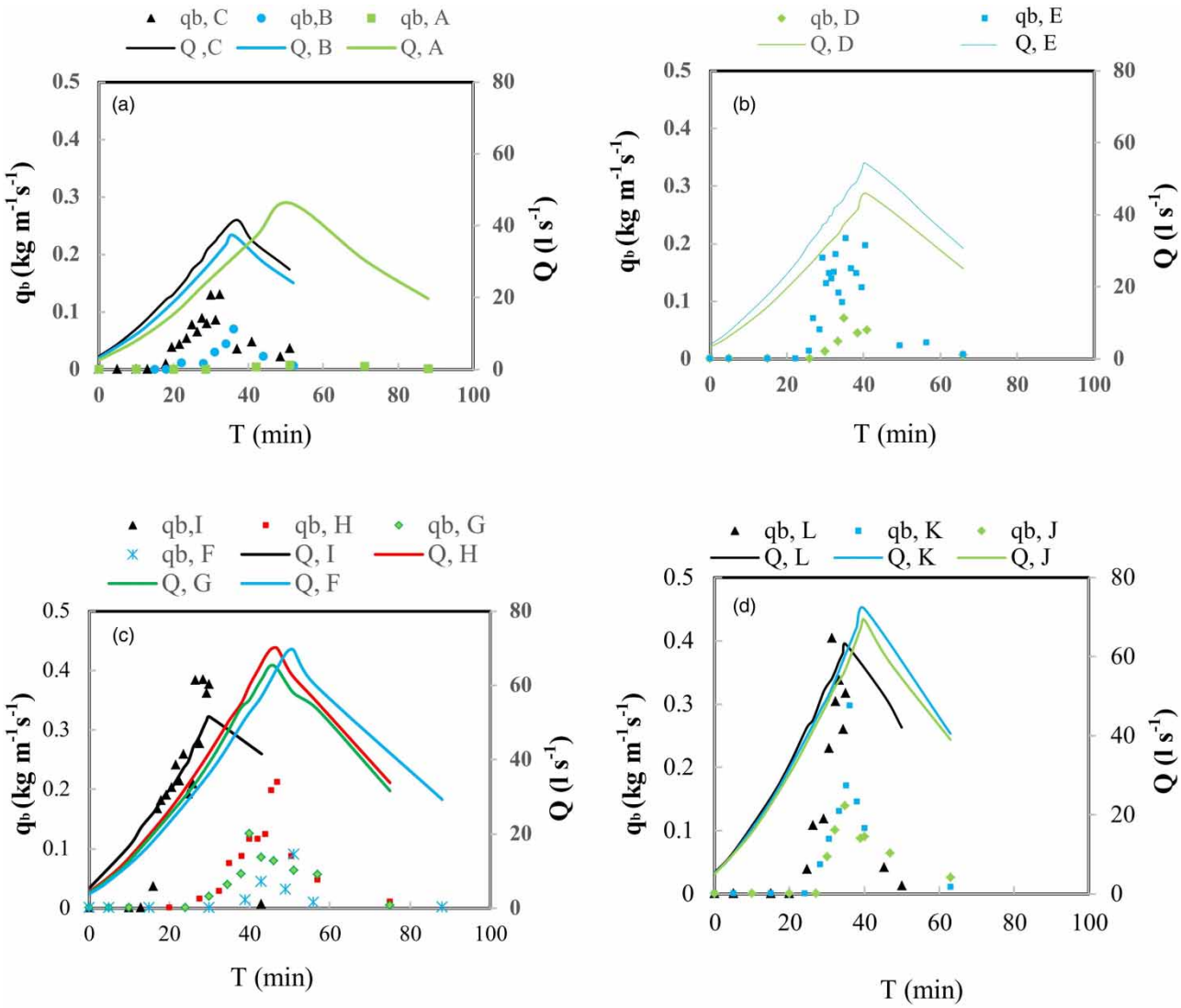

Figure 2 | Temporal variation of sediment transport rate for runs conducted using different sizes of uniform grains: (a) $D = 5.17$ mm; (b) $D = 10.35$ mm; (c) $D = 14$ mm; and (d) $D = 20.7$ mm.

0.015 m m^{-1}, the maximum and minimum fractional sediment transport rates occurred for the 14 mm and the 5.17 mm fractions, respectively. The ratio of the fractional sediment transport rates (5.17, 10.35, 14, and 20.7 mm) to the total sediment transport rate were 0.079, 0.29, 0.33, and 0.3, respectively.

Temporal lag between sediment transport and discharge

The temporal lag between the peaks of discharge and sediment transport rates was investigated by transforming the variables into dimensionless terms, i.e., Einstein bed load parameter (q_b*), dimensionless base time, (t*), and dimensionless discharge (Q*) by intense sampling of transported sediment around the peak of discharge.

Results of the lag time between the hydrograph peak and sediment shows that the lag time has been increased with increasing bed slope for all uniform and graded bed sediment conditions except for the case of uniform coarse sediment of 20.7 mm, which shows the opposite trend (Figure 5). One possible reason could be that since finer sediment is transported more easily, an increase in bed slope results in a huge amount of sediment

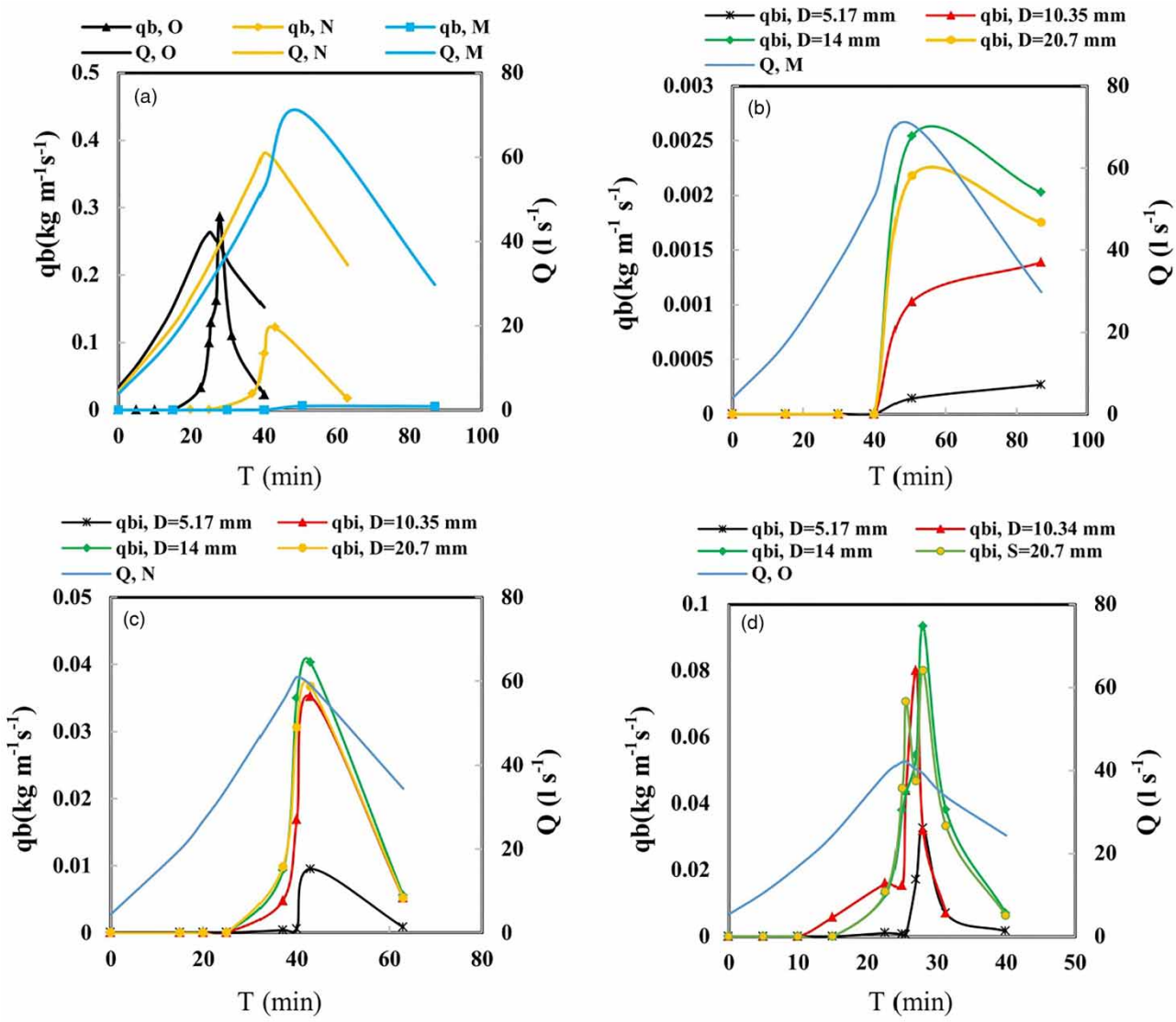

Figure 3 | Temporal variation of transport rates for experiments conducted using the graded bed sediment: (a) total transport rate at $S = 0.015$, 0.02, and 0.03; (b) fractional transport rate at $S = 0.015$ m m^{-1}; (c) fractional transport rate at $S = 0.02$ m m^{-1}; (d) fractional transport rate at $S = 0.03$ m m^{-1}.

transported in a low flow depth. Thus, sediment transport is reduced for higher flow depths due to armoring and lower sediment budget (sediment transport is a function of sediment budget (Asselman 1999)). As coarser particles are not transported as easily, their transport is consistent with slope and flow depth and this transport capacity is increased with an increase in both bed slope and flow depth.

The main differences between the uniform and graded bed sediment is that the peak of the uniform bed sediment transport rate occurred before the peak of the hydrograph, whereas in all tests using graded sediments, the peak of total graded sediment transport rate occurred on the recession limb of the hydrograph (Figures 2 and 3).

Comparison of bed load transport rates between experiments conducted using homogenous versus graded sediments

At a slope of 0.015 m m^{-1} the dimensionless bed load sediment transport rates for the 10.35 mm and 14 mm

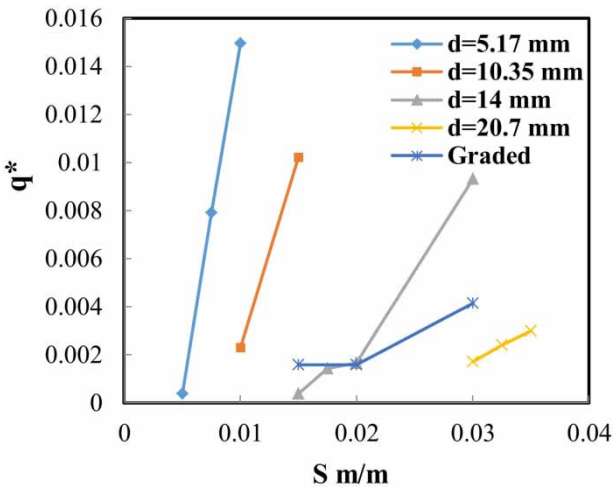

Figure 4 | q^* as a function of bed slope for graded and uniform bed sediment.

Table 4 | Ratio of total weights of transported uniform sediment per graded

Ratio of total weights of transported uniform sediment per graded	$S = 0.015$	0.02	0.03
10.35 mm/graded	25.42	–	–
14 mm/graded	3.10	1.13	0.74
20.7 mm/graded	–	–	0.76

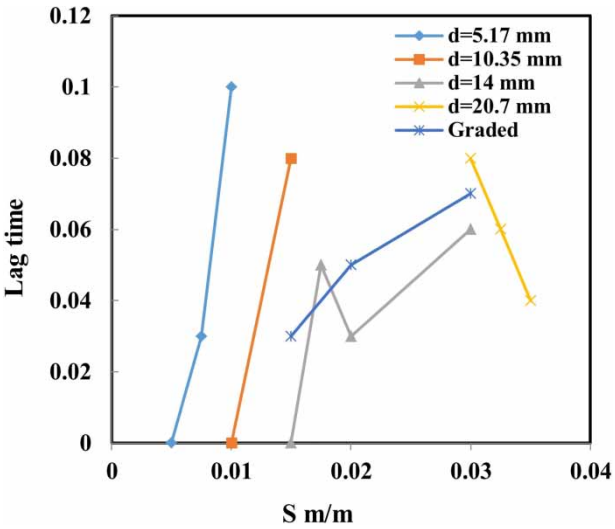

Figure 5 | Lag time between peak of flow and sediment as a function of bed slope.

fractions were 99% and 80% lower than their uniform counterparts, respectively. Whereas at a slope of 0.02 m m^{-1} and a peak discharge of 70 l s^{-1}, the dimensionless bed load sediment transport rates for the uniform and 14 mm fractions are closer (19% lower). It shows that by increasing the bed slope the transported fraction particles in a graded bed sediment were closer to their uniform counterparts. For the coarse sediment of size 20.7 mm the opposite trend is observed. With a slope of 0.03 m m^{-1}, the finer fractions (i.e., 5.17, 10.35, and 14 mm) cause the coarse fraction of 20.7 mm to be transported at 64% higher compared to their uniform counterparts. Results also show that transport rate peak for the 10.35 and 14 mm uniform bed sediment occurred earlier compared to their fraction counterparts, but the opposite case was observed for the coarse sediment of 20.7 mm as the peak transport rate of the fraction occurred earlier compared to their uniform counterparts (Figure 6).

Patterns of hysteresis

Because the discharge and coarse sediment transport rates can peak at different times during the simulated hydrographs, a plot of these two variables was created to illustrate the hysteretic pattern. The patterns would be clockwise if the discharge peaks after the sediment transport rate, or counterclockwise if the discharge peaks before the sediment transport rate (Mao 2012; Guney *et al.* 2013). Generally, uniform bed sediments have a clockwise hysteresis, but graded bed sediment follows the counterclockwise hysteresis pattern (Figure 7).

Fractional sediment mobility

Figure 8(a)–8(c) show the temporal variation in fractional bed load mobility parameter (Ψi) for graded sediment. Generally, finer fractions increased and coarser fractions severely reduced the mobility on the recession limb of the hydrograph. The opposite trend was observed on the rising limb. Results also show that with increasing bed slope, the mobility of the fine fraction (e.g., 5.17 and 10.35 mm) has reduced and the mobility of the coarse fraction (e.g., 14 and 20.7 mm) is increased during the rising limb. The opposite trend was observed in the recession limb (Figure 9(a) and 9(b). As in the recession limb with an increasing bed slope from 0.015 to 0.03 mm^{-1}, the mobility of the 5.17 and 20.7 mm fractions became

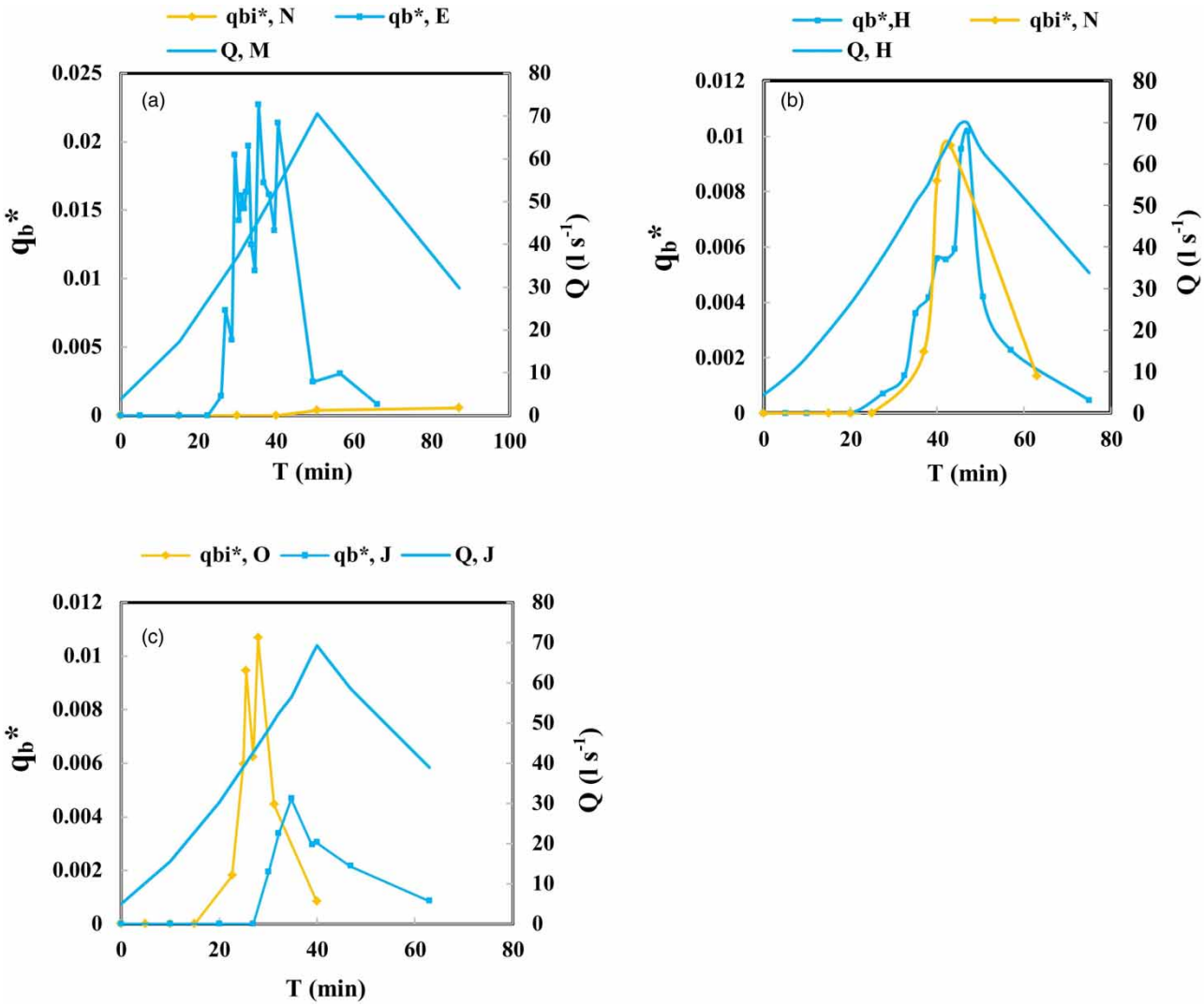

Figure 6 | Temporal variation in q_b* for graded and uniform bed sediment during the passage of the hydrograph: (a) $D = 10.35$; (b) $D = 14$; and (c) $D = 20.7$ mm.

0.4 and 1.3 times, but these are 2.8 and 0.8 times respectively in the falling limb. Results revealed that in the rising limb, with increasing bed slope, the coarser the fraction, the higher the mobility; in the bed slope of 0.015 m m^{-1} the higher mobility was that of 14 mm but in the slope of 0.03 it was that of 20.7 mm. The mobility of 20.7 and 14 mm fractions in the slope of 0.03 m m^{-1} is 1.2 and 1.04 times, respectively.

A further way to visualize the mobility of sediment fractions along the hydrographs is to draw the grain-size curves of sediment samples collected in traps during the runs. Figure 10 shows that the grain-size curves for the rising limb plot towards the right, which indicate that the transported sediments were coarser compared to the original sediment grain size distribution. The curves corresponding to samples taken during the recession limb plot to the left, which indicate that the transported sediments were finer than the grain size distribution of sediment in transport during the rising limb. At a slope of 0.03 m m^{-1} the median size of the sediment mixture (D_{s50}) was equal to 12.5 mm, but the median size of transported sediments (D_{b50}) was 17.1, 17.9, and 19.3 mm on the rising limb and

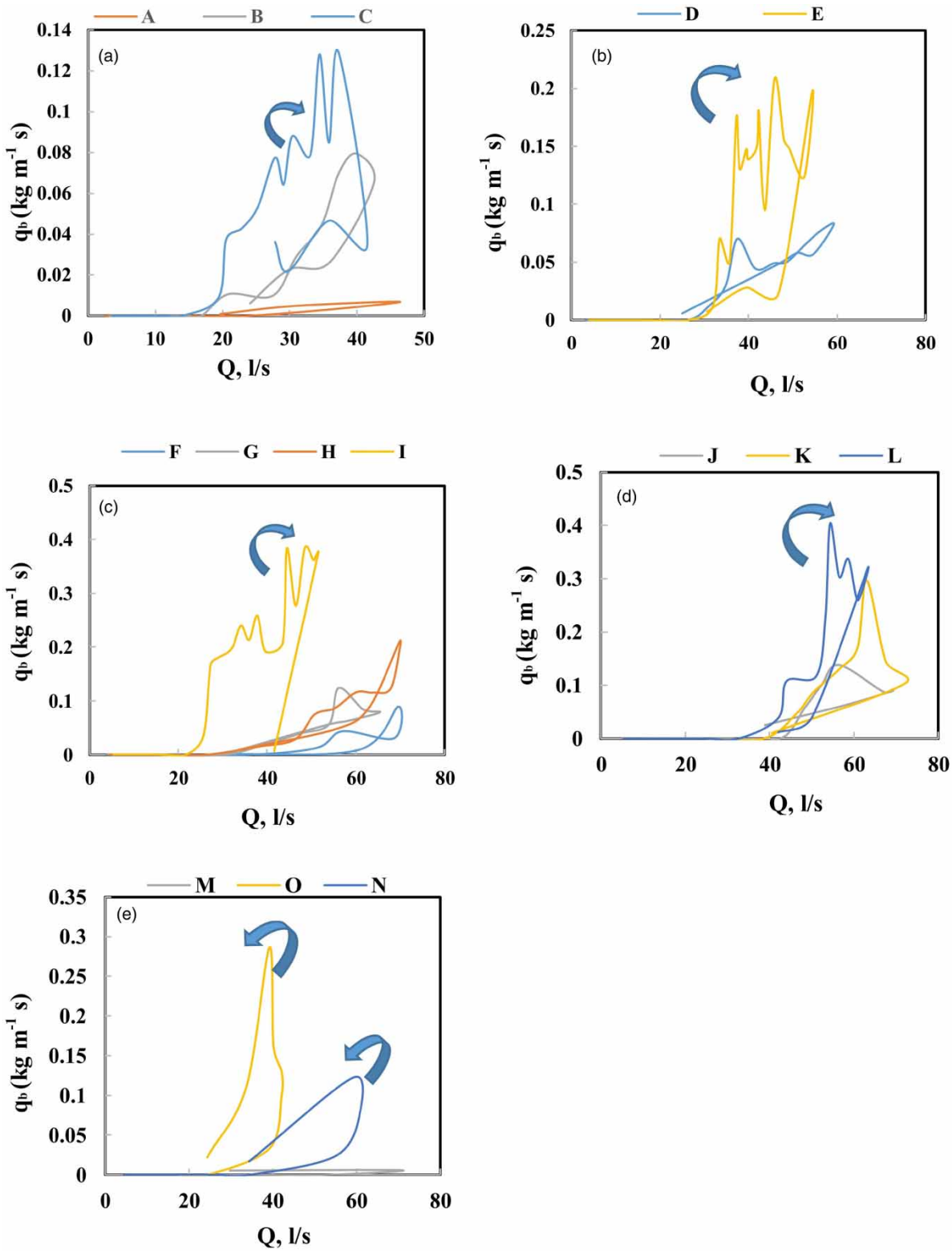

Figure 7 | Hysteresis loop for experiments conducted using different grain sizes: (a) $D = 5.17$ mm; (b) $D = 10.35$ mm; (c) $D = 14$ mm; (d) $D = 20.7$ mm; (e) $D =$ graded mixture.

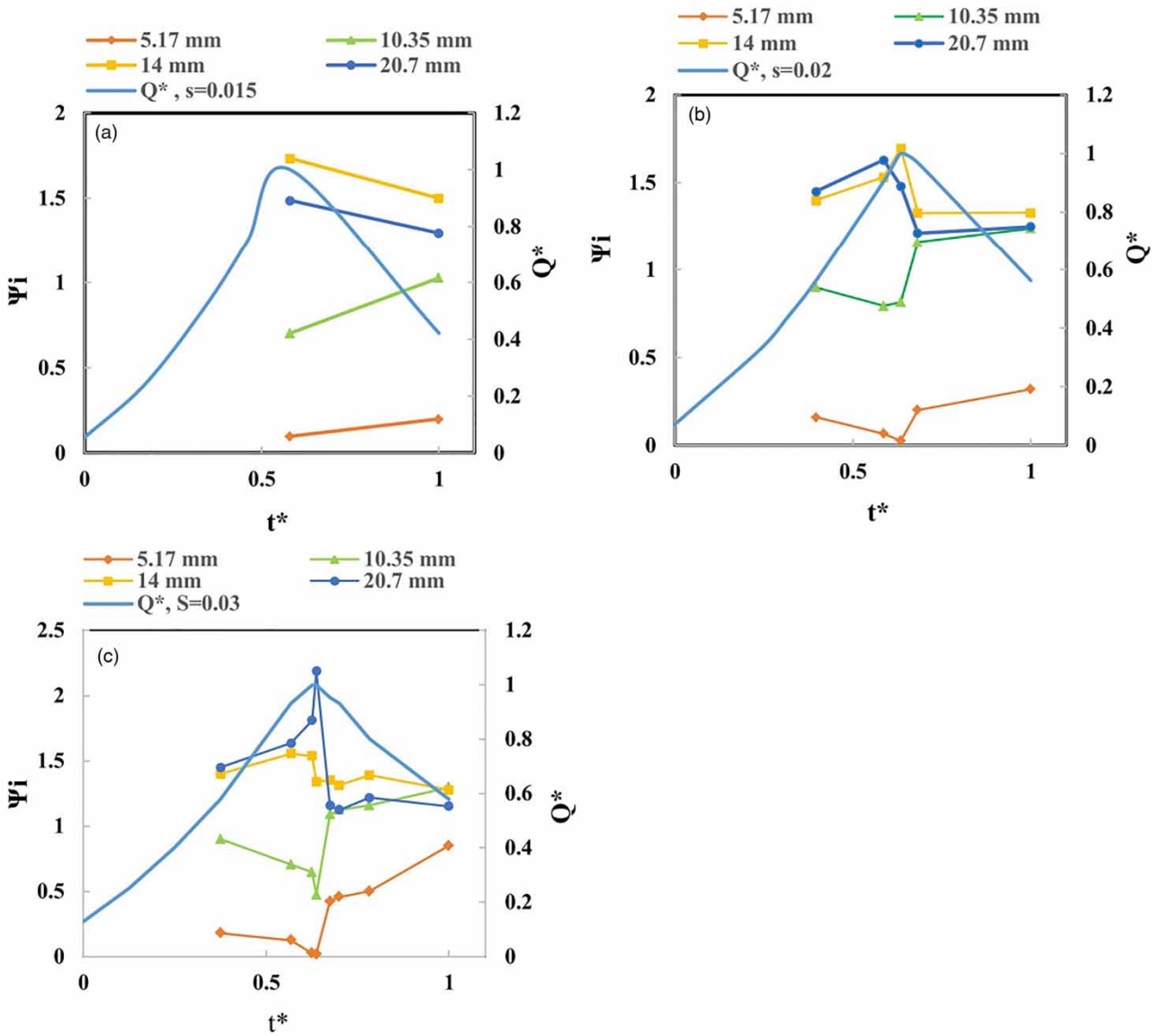

Figure 8 | Fractional bed load mobility: (a) S = 0.015; (b) S = 0.02; and (c) S = 0.03.

14.5, 14.3, and 14.2 mm on the recession limb. Although D_{b50} reduced in the recession limb, the median size of the transported sediment (D_{b50}) was higher than the median size of the sediment mixture (D_{s50}) on both the rising and recession limbs of the hydrograph.

Relationship between q^* and Shield stress

In the literature, the relationship between q^* and Shield stress was investigated for low Einstein sediment transport (lower than 0.001) especially for uniform flow conditions (i.e., Shvidchenko & Pender 2000; Shvidchenko *et al.* 2001). The relationship was determined to be near linear. However, for high Einstein bed load parameter value under unsteady flow conditions which is rarely addressed, the result shows that for $q^* > 0.001$ the relationship between q^* and Shield stress is logarithmic and with changes in the bed slope, the change in Shield stress is more apparent and significant than q^* (Figure 11).

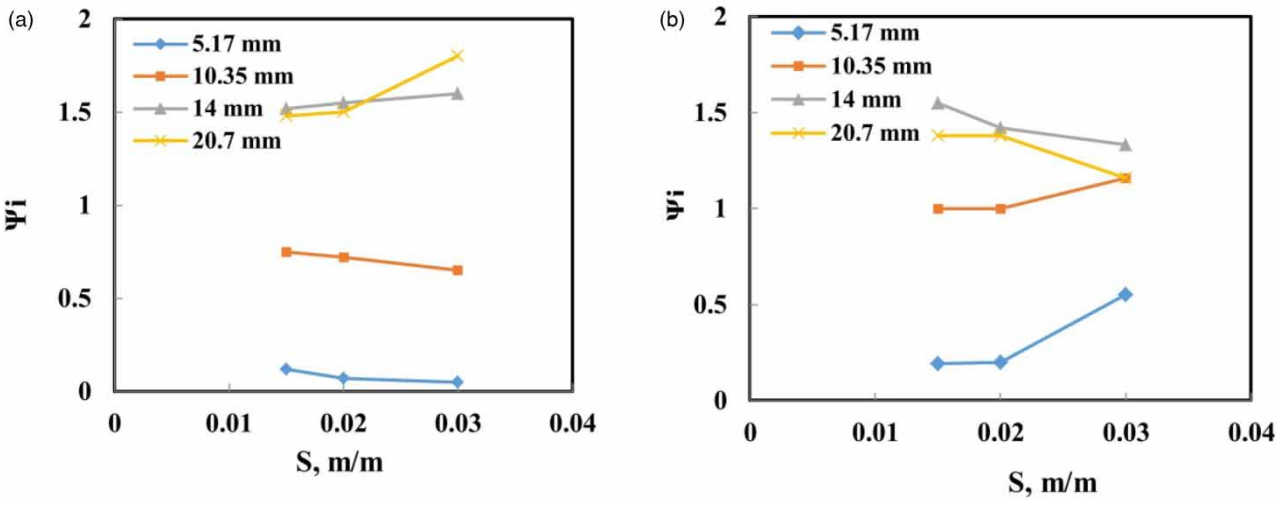

Figure 9 | Fractional bed load mobility with bed slope: (a) raising limb; (b) falling limb.

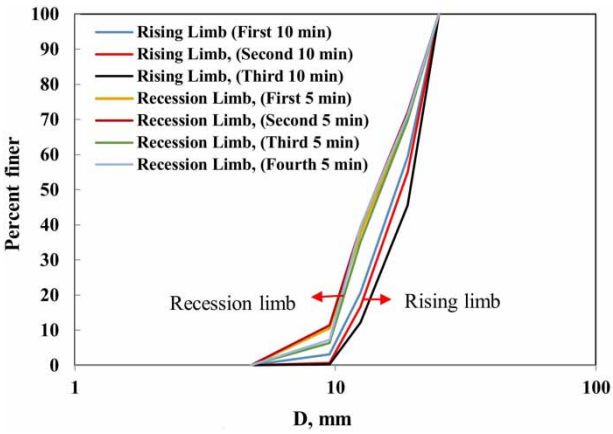

Figure 10 | The change in transported grain size with the recession and falling limb of the hydrograph.

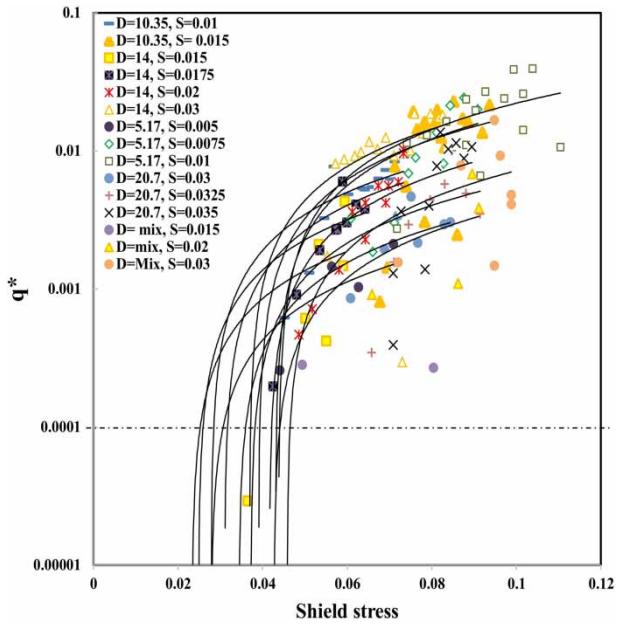

Figure 11 | Relationship between q^* and Shield stress for unsteady flow in degrading channel.

DISCUSSION

Temporal variation in bedload sediment transport rate

Temporal variation of uniform bed sediment showed that for slopes smaller than 0.0075 m m^{-1}, the peak of sediment transport rate occurred coincidently with the peak of flow discharge. However, for higher slopes, the peak of sediment took place earlier than flow peak. This may be due to the fact that at higher bed slopes, the grains composing the surface layer structured during the first portion of the rising limb of the hydrograph become dislodged before the arrival of the hydrograph peak, creating an early pulse of sediment flux (clockwise hysteresis).

In the graded bed sediment, the proportions of the sediment transport rate for fractions of 5.17, 10.35, 14, and 20.7 mm to the total sediment transport rate on a slope of 0.015 m m^{-1} were 0.044, 0.23, 0.42, and 0.35, respectively. The maximum transport rate for 5.17 and 10.35 mm

fractions took place after the peak discharge, while it happened before the peak discharge for 14.0 and 20.7 mm particles. Bed load sediment transport rate for 5.17 and 10.35 mm fractions after the peak discharge was ascending and for 14 and 20.7 mm fractions it was descending. This reveals that the peak of finer fractions occurred after the peak discharge (in the recession limb) and for the coarser fraction it was before the peak discharge (in the rising limb), which is in agreement with the results obtained by Wang *et al.* (2015) on experiments conducted at a slope of 0.0083 m m^{-1}.

The proportions of the sediment transport rate for fractions of 5.17, 10.35, 14.0, and 20.7 mm to the total sediment transport rate on a slope of 0.03 were 0.2, 0.5, 0.56, and 0.5, respectively. For this slope, unlike the slope 0.015 m m^{-1}, peaks of all fractions occurred after the peak discharge on the recession limb. This may be due to the fact that with the increase in bed slope, the armor layer can break up more easily due to increased shear stress and cause peaks to be reached after the peak of flow. Also the more the amount of coarser fraction that moved through the rising limb, in the recession limb we expect to have a greater amount of bed movement due to having the finer bed material in the recession limb.

For grain fractions of 5.17, 10.35, 14, 20.7 mm and total value, by increasing the slope to 1.5 times (compared to 0.02 m m^{-1}), the amounts of q^* were 3.4, 2.3, 2.29, 2.0, and 2.66, respectively, and also by doubling the slope (related to slope of 0.015), the value of q^* were 154, 62.5, 51, 52, and 72 times larger, respectively. This comparison suggests that, in graded sediments, an increase in bed slope led to the increase in the mobility of finer fractions during the recession limb. However, as shown in Figure 5, the peak of fractions occurred simultaneously in the same time as the total mixture sediment.

Comparing bedload transport rates between experiments conducted using homogenous and graded sediments, the results suggest that coarser grain size fractions in the graded bed sediment have greater mobility compared to the same grain size in uniform mixtures. The reason is mainly that: (1) the coarse sediments in the graded sediment are more exposed to the flow; and (2) fine fractions increased the transport rate of coarse fractions compared to uniform sediment which is in accordance with the findings of Mao (2012), Wang *et al.* (2015), and Li *et al.* (2016, 2018). Also, a comparison between the sediment transport peaks of uniform sediments and individual fractions revealed that, because the fine fractions are hidden behind coarse fractions in graded sediment mixtures, the peak of finer fractions occurred later than their uniform size counterparts and the coarser fractions had an earlier peak than their uniform size counterparts due to increased exposure. Hence, this concealment had a significant effect on sediment transport in graded sediment mixtures and affected the temporal lag between different fractions and their uniform sediment counterparts.

Results of the changes in the mobility for each fraction in both rising and recession limb are in accordance with the results of Hassan *et al.* (2006) who revealed that in the falling limb of an asymmetrical hydrograph the transport of fractions coarser than 2.8 mm stopped but in the rising limb fractions coarser than 11 mm had higher mobility.

Hysteretic patterns of sediment transport during hydrographs

Bedload clockwise hysteresis loops occur when the sediment transport rate peaks before the peak discharge of the hydrograph and a counterclockwise pattern occurs when the sediment transport rate peak takes place after the peak discharge of the hydrograph. In the present study, complex figure eight-shaped loops were generally observed in the runs, because sediment discharge fluctuated along the rising hydrograph limb in high discharge and slope conditions, and generally did not follow the ascending trend and acted similarly to a multi-peak hydrograph, and as a result, formed as the figure eight-shaped pattern. With the increase in the bed slope or flow discharge, the sediment transport rate increased in a manner consistent with the increase in bed slope. However, on very high and steep slopes the bed would be unstable (resulting in a completely degraded channel) and there was a high rate of bed erosion. The sediment transport rate over time had a sinusoidal shape, and with increase of flow discharge and low and high transport rates continued through to the peak of hydrograph (anti-dunes moving upstream were observed). On the other hand, with the flow reducing on the recession limb, this sinusoidal shape rate ended and sediment

transport rate reduced. Mao (2012) stated that in high discharge conditions, the sediment transport rate fluctuated during the rising limb of the hydrograph; the amount and intensity of the fluctuations observed in the rising limb of the hydrographs in the present runs were severe and, thus, the loops act similarly to multi-peak discharge conditions for steep slopes.

Hysteresis in both clockwise (Humphries *et al.* 2012) and counterclockwise (Lee *et al.* 2004) directions has been observed in flume experiments, most of which were related to the temporal lag of upstream sediment conditions and the passage of bed forms or sediment pulses (Mao 2012). As shown in Figures 2–4, there was always a temporal lag between peaks of flow and sediment discharge, and the loop patterns resulting from this delay are shown in Figure 7(a)–7(f). The effect and shape of loops are important indicators for various processes of runoff and sediment sources and transport (Seeger *et al.* 2004; Krueger *et al.* 2009; Eder *et al.* 2010). In the current study, experiments were performed with zero feeding of sediments upstream, and thus, the observed counterclockwise pattern can be ascribed to the progressive armouring of the bed, and to the fact that transported sediments becomes progressively finer during the falling limb of the hydrographs (as the coarser sediments are transported mainly before the arrival of the peak discharge). Guney *et al.* (2013) showed that hysteresis is initially clockwise but after the development of an armor layer it changed to a counterclockwise pattern.

Impact of hydrograph characteristics on the total bedload sediment transport

The impact of some hydrograph characteristics, such as the unsteadiness parameter, symmetry parameter, and total water work parameter, on the dimensionless bedload sediment transport rate parameter of the total and fractional grain sizes is shown in Table 2 and Figure 12. It was observed that the transported sediment increased with increase in W_k, meaning that an increase in the maximum volume under the hydrograph resulted in an increase in sediment transport. The sediment transport rate also increased with reduction in W_k and an increase in bed slope (shear stress or relative roughness) demonstrated a higher impact on the sediment transport rate compared to

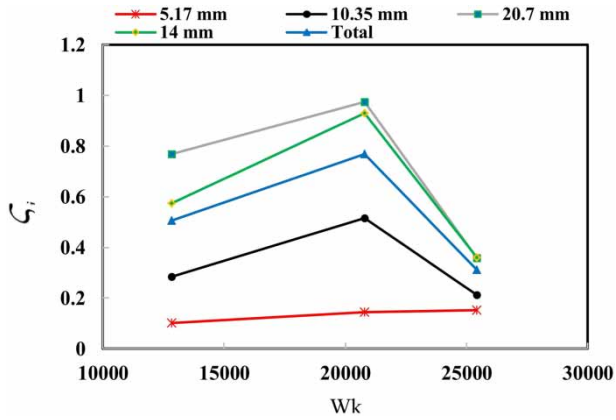

Figure 12 | Variation of ς versus W_k for fractions in graded sediment.

the volume under the hydrograph. To investigate the effect of flow and bed characteristics on uniform, total, and fractional sediment transport on the rising and recession limbs, the relative transport yield ratio was computed following Wang (2016) as:

$$\varsigma = \frac{Wt_R}{Wt_F} \text{ and } \varsigma_i = \frac{Wti_R}{Wti_F} \tag{11}$$

where R is for the rising limb, and F is for the recession limb. Clearly, this fraction was more than 1 for higher sediment transport rates occurring on the rising limb and less than 1 for higher sediment transport rates occurring on the recession limb.

One factor that was observed in most cases, but that cannot necessarily be generalized and needs further investigation, is that the relative transport yield ratio increased with increasing bed slope, meaning that the sediment transport rate on the rising limb of the hydrograph increased compared to the recession limb of the hydrograph for an increasing bed slope. The relative transport yield ratio was more than 1 for uniform particles, showing that the transported sediment was higher during the rising limb of the hydrograph in all cases, which is due to the fact that no sediment was fed during the experiments. The relative transport yield ratio was less than 1 for the graded sediment in three runs showing that the transported sediment on the recession limb of the hydrograph was higher compared to the rising limb of the hydrograph. This is in accordance with the result of Guney *et al.* (2013) and opposite to the

findings of Wang *et al.* (2015) for graded sediment. The mechanism behind this result is still unclear (Li *et al.* 2018). Some researchers (e.g., Mao 2012; Li *et al.* 2018) show that sediment transport on the rising limb is greater compared to the falling limb for graded sediment, and others (Lee *et al.* 2004) for uniform and Guney *et al.* (2013) for graded sediment show the opposite result. Also, Kuhnel (1992) determined that the sediment transport rate in the falling limb of the hydrograph is greater compared to the raising limb of the hydrograph for low flows and the opposite for high discharge conditions. Also, Mao (2012) stated that the differences in the sediment transport rates during the rising and falling limb of the hydrograph is due to the different grain sizes of the transported sediment. Similar dynamics are evident in the present experiments as, for graded sediment, coarser fractions are more mobile during the rising limb, and as the bed becomes finer in response to this transport, finer sediment were transported during the recession limb of the hydrograph. Alternatively, this may be a result of the higher shear stresses and therefore breaking of the armor layer for the graded sediments.

Hence, uniform and graded sediment acted in opposite fashions. According to Hassan *et al.* (2006), rivers experiencing floods with short falling limbs (i.e., about 1 hour) are less likely to develop a strong armor, thus, there is not enough time for vertical winnowing of finer sediments into the coarser framework of the bed. Also, Hassan *et al.* (2006) inferred from their experiments that, since winnowing is not responsible for the development of armoring in rivers with flash floods (i.e., in arid environments), the hysteresis is due to the size of the transported material or morphodynamic factors. In the present study, short hydrographs do not develop evident armoring either, and therefore, hysteresis is weak due to the large amount of fine sediment moved during the falling limb of the hydrograph.

Another finding, shown in Figure 12, is that in graded sediment, the coarser the fractions, the more the relative transport yield ratio. Hence, the 20.7 mm fraction had the highest relative transport yield ratio, followed by 14.0, 10.35, and 5.17 mm fractions. The amount of ς for the 20.7 and 14.0 mm fractions was greater than the amount of total sediment and for 10.35 and 5.17 mm fractions it was lower than the amount of total sediment, showing higher transport of coarser fraction, which is potentially due to reduced availability of fine fractions from the surface and resulting from this fact the coarse (fine) fractions are more prone to exposure (hiding) dynamics.

It should be noted, it may be that Figures 8 and 12 appear not to be in harmony with each other, as if the coarse sediment has an increased mobility, and thus this may be why ς_i is less than 1 for coarse fractions. It can be stated that there are different methods of calculation, such as in the mobility index, the proportion of each fraction in the trap was divided per proportion of those fractions in the original bed. However, for ς_i, only the weights of the rising limb are divided per the falling and as the weights of the falling limb are more than the rising, for all fractions the ς_i is less than 1.

Regarding sediment mobility during the hydrographs, it should be noted that the mobility of coarser fractions is increased during the rising limb and reduced during the falling limb. For fine materials, the opposite is true, as the mobility of fine fractions in the rising and falling limbs of the hydrograph are reduced and increased, respectively. These results are in accordance with results of Hassan *et al.* (2006), which revealed that during the falling limb of an asymmetrical hydrograph the transport of the fractions coarser than 2.8 mm was stopped but in the rising limb the fractions coarser than 11 mm had higher mobility. Wang *et al.* (2015) reported similar results. The result may be due to lack of sediment feeding. In the present study, the transported sediment in both rising and falling limbs is generally coarser than the original bed sediment which could be due to the protrusion of coarser fractions or the concealment of finer fractions, which is the opposite of the result of Hassan *et al.* (2006).

One more important issue is that, as finer particles cause higher sediment transport rates, it is vital to manage the upstream region of the catchment using watershed management practices such as constructing check-dams, buffer strips, afforestation, or control areas with high extreme soil erosion rates like agriculture land with the use of catch crops, straw, and so on. These measures play a useful role in reducing river morphological changes (Cerdà *et al.* 2018; Rodrigo-Comino *et al.* 2018).

One of the main limitations of the present study is that sediment particles were considered cohesionless, but in general, sediment in natural rivers is not cohesionless and

contains some silt and other fine particles. Thus, for future work, it is suggested to use mixed materials with more fractions (ranging from cohesive to non-cohesive particles) and equal proportions of mixed grain sizes in hydrographs with longer base time to realize the real mobility of fractions during long-term flood events.

Generally, the results of the present study provide a greater understanding of the transport of graded bed sediments in comparison to their uniform bed sediment transport counterparts in response to flood events and insights for improved numerical modeling capabilities for bedload sediment transport.

CONCLUSION

The bed sediment response to a natural hydrograph of flow during flooding was studied for uniform sediment particles and also mixtures of uniform sediment with equal weight ratios on bed slopes ranging from 0.005 to 0.035 m m^{-1}. In addition to the total amount of sediment transport, the temporal variation of bed sediment transport, mobility of fractions, relative transport yield ratio as well as temporal lag between the peaks of flow and sediment were also studied.

Results showed that for a given grain size, the increase in bed slope increased the Einstein bedload parameter and Shields stress. More importantly, for a change in the slope, the change in the Einstein bed load parameter was lower than that in the Shields stress. Results of analysis of the temporal variation and sediment transport rates showed that for uniform particles, the peak of sediment transport occurred before the peak of flow; but for fraction particles in the graded sediment, the peak of fine fractions occurred after the peak of flow discharge and for coarse fractions occurred before the peak of flow, which was not the case on slopes steeper than 0.015 m m^{-1}. Results of the fractions in terms of bed mobility parameter and grading curve showed that the mobility of coarser fractions increased on the rising limb of the hydrograph and reduced on the recession limb as the trend was opposite for fine fractions, but the amount of transported sediment was higher than the bed sediment surface on both rising and recession limbs.

Comparison between fractions and their uniform particle counterparts showed that the fine fraction sediment transport rate was less than their uniform particle counterparts, but the amount of coarser fraction sediment transport rate was higher than for their uniform sediment transport rate counterparts. In addition, the coarser fraction in graded sediment mixtures caused a reduction in the finer fraction bed load sediment transport rate, and the finer fraction caused an increase in the coarser fraction bed load sediment transport rate than their uniform particle counterparts.

The measured sediment transport rate for uniform and graded sediments showed that there was a temporal lag between peaks of flow and sediment that varied from 0.02 to 0.10 base time of the hydrograph. To compare the temporal lag between the peaks of uniform and fractions of sediments, it was concluded that due to the concealment effect of finer fractions, the peak of finer fractions occurred after the peak of the uniform sediment transport rate counterparts, but is opposite for coarser fractions. For finer particles of 5.17 and 10.35 mm and also for the graded sediment mixture, the time interval between peaks of flow and sediment increased with increasing bed slope but the coarser fraction (14.0 and 20.7 mm) behaved oppositely. The relative transport yield ratio was always more than 1 but less than 1 for uniform and graded sediments, respectively. In the graded bed sediment mixture on the same slope, coarser fractions resulted in higher relative transport yield ratios. In general, uniform particles had a clockwise hysteresis loop and graded sediment had a counterclockwise hysteresis loop.

REFERENCES

Asselman, N. E. M. 1999 Suspended sediment dynamics in a large basin: the river rhine. *Hydrological Processes* **13**, 1437–1450.

Bagnold, R. A. 1966 An approach to the sediment transport problem from general physics. *USGS* **422**, 280–283.

Barati, R. & Salehi Neyshabouri, S. A. A. 2019 Discussion of evaluation of bed load equations using field-measured bed load and bed material load by Sanjay kumar Madhusudan Yadav, Vipin Kumar Yadav, and Anurag Gilitwala. *ISH Journal of Hydraulic Engineering* **25**, 1–3.

Barati, R., Neyshabouri, S. S. & Ahmadi, G. 2014 Numerical simulation of the sediment transport in the saltation regime. In: *River Flow 2014: Proceedings of the International Conference*, Lausanne, Switzerland.

Barati, R., Neyshabouri, S. A. A. S. & Ahmadi, G. 2018 Issues in Eulerian-Lagrangian modeling of sediment transport under

saltation regime. *International Journal of Sediment Research* **33** (4), 441–461.

Bell, R. G. & Sutherland, A. J. 1983 Non-equilibrium bed-load transport by steady flows. *Journal of Hydraulic Engineering* **109**, 351–367. doi:10.1061/(ASCE) 0733-9429(1983)109:3(351).

Berta, A. M. & Bianco, G. 2010 An expression for the water-sediment moving layer in unsteady flows valid for open channels and embankments. *Natural Hazards and Earth System Science* **10** (5), 1051–1059.

Bombar, G., Elçi, Ş., Tayfur, G., Güney, M. Ş. & Bor, A. 2011 Experimental and numerical investigation of bed-load transport under unsteady flows. *Journal of Hydraulic Engineering* **137** (10), 1276–1282.

Cerdà, A., Rodrigo-Comino, J., Giménez-Morera, A. & Keesstra, S. D. 2018 Hydrological and erosional impact and farmer's perception on catch crops and weeds in citrus organic farming in Canyoles river watershed, Eastern Spain. *Agriculture, Ecosystems & Environment* **258**, 49–58.

Chien, N. & Wan, Z. 1999 *Mechanics of Sediment Transport*. ASCE Press, Reston, VA, USA.

Chien, N., Zhou, Z. & Zhang, R. 1987 *River Process*. Chinese Science Press, Beijing, China.

Church, M. 2006 Bed material transport and the morphology of alluvial rivers. *Annual Review of Earth and Planetary Sciences* **34** (1), 325–354.

De Sutter, R., Verhoeven, R. & Krein, A. 2001 Simulation of sediment transport during flood events: laboratory work and field experiments. *Hydrological Science Journal* **46** (4), 599–610.

Eder, A., Strauss, P., Krueger, T. & Quinton, J. N. 2010 Comparative calculation of suspended sediment loads with respect to hysteresis effects (in the Petzenkichen Catchment, Austria). *Journal of Hydrology* **389** (1), 168–176.

Graf, W. H. & Qu, Z. 2004 Flood hydrographs in open channels. *Proceedings of the Institution of Civil Engineers-Water Management* **157** (1), 45–52.

Graf, W. H. & Suszka, L. 1985 Unsteady flow and its effect on sediment transport. In: *Proceedings of 21st IAHR Congress*, Melbourne, Australia.

Guney, M. S., Bombar, G. & Aksoy, A. O. 2013 Experimental study of the coarse surface development effect on the bimodal bedload transport under unsteady flow conditions. *Journal of Hydraulic Engineering-ASCE* **139** (1), 12–21.

Habersack, H. M., Nachtnebel, H. P. & Laronne, J. B. 2001 The continuous measurement of bed load discharge in a large alpine gravel bed river. *Journal of Hydraulic Research* **39**, 125–133. doi:10.1080/00221680109499813.

Hassan, M., Egzoy, R. & Parker, G. 2006 Experimental on the effect of hydrograph characteristics on vertical grain sorting in gravel bed rivers. *Water Resources Research* **42** (9), 1–15.

Humphries, R., Venditti, J. G., Sklar, L. S. & Wooster, J. K. 2012 Experimental evidence for the effect of hydrographs on sediment pulse dynamics in gravel-bedded rivers. *Water Resource Research* **48** (1). doi:10.1029/2011WR010419.

Huygens, M., Verhoeven, R. & De Sutter, R. 2000 Integrated river management of a small Flemish river catchment. In: *The Role of Erosion and Sediment Transport in Nutrient and Contaminant Transfer, Proceedings of Symposium*, Waterloo, Canada, pp. 191–198. IAHS Publ. No. 263.

Karimaee Tabarestani, M. & Zarrati, A. R. 2014 Sediment transport during flood event: a review. *International Journal of Environmental Science and Technology* **12** (2), 775–788.

Keesstra, S., Nunes, J. P., Saco, P., Parsons, T., Poeppl, R., Masselink, R. & Cerdà, A. 2018 The way forward: can connectivity be useful to design better measuring and modelling schemes for water and sediment dynamics? *Science of the Total Environment* **644**, 1557–1572.

Keesstra, S. D., Davis, J., Masselink, R. H., Casalí, J., Peeters, E. T. & Dijksma, R. 2019 Coupling hysteresis analysis with sediment and hydrological connectivity in three agricultural catchments in Navarre, Spain. *Journal of Soils and Sediments* **19** (3), 1598–1612.

Klein, M. 1984 Anti-clockwise hysteresis in suspended sediment concentration during individual storms: Holbeck Catchment; Yorkshire, England. *Catena* **11** (2), 251–257.

Krueger, T., Quinton, J. N., Freer, J., Macleod, C. J., Bilotta, G. S., Brazier, R. E., Butler, P. & Haygarth, P. M. 2009 Uncertainties in data and models to describe event dynamics of agricultural sediment and phosphorus transfer. *Journal of Environmental Quality* **38**, 1137–1148.

Kuhnle, R. A. 1992 Bed load transport during rising and falling stages on two small streams. *Earth Surface Processes and Landform* **17**, 191–197. doi:10.1002/esp.3290170206.

Lee, K. T., Liu, Y. L. & Cheng, K. H. 2004 Experimental investigation of bed load transport processes under unsteady flow conditions. *Hydrological Processes* **18** (13), 2439–2454.

Lenzi, M. A. & Marchi, L. 2000 Suspended sediment load during floods in a small stream of the Dolomites (northeastern Italy). *Catena* **39**, 267–282.

Li, Z., Cao, Z., Liu, H. & Pender, G. 2016 Graded and uniform bed load sediment transport in a degrading channel. *International Journal of Sediment Research* **31**, 376–385. DOI: 10.1016/j.ijsrc.2016.01.004.

Li, Z., Qian, H., Cao, Z., Liu, H., Pender, G. & Hu, P. 2018 Enhanced bed load sediment by unsteady flows in a degrading channel. *International Journal of Sediment Research* **33** (3), 327–339.

Mao, L. 2012 The effect of hydrographs on bed load transport and bed sediment spatial arrangement. *Journal of Geoscience and Research* **117**, 374–386.

Mrokowska, M. M. & Rowinski, P. M. 2019 Impact of unsteady flow events on bed load transport: a review of laboratory experiment. *Water* **11**, 907. doi:10.3390/w11050907.

Nouh, M. 1988 Method of estimating of bedload transport rates applied to ephemeral stream. In: *Sediment Budgets, Proceedings of the Porto Alegre Symposium*. IAHS Publication, Vol. 174, pp. 97–106.

Parker, G. & Klingeman, P. C. 1982 On why gravel bed streams are paved. *Water Resources Research* **18** (5), 1409–1423.

Parker, G., Hassan, M. & Wilcock, P. 2007 Adjustment of the bed surface size distribution of gravel-bed rivers in response to cycled hydrographs. *Developments in Earth Surface Processes* **11**, 241–285.

Pathirana, K., Ranasinghe, K. & Ratnayake, U. 2006 Bed shear stress in unsteady open channel flow over rough beds. *Journal of the Chinese Institute of Engineering* **41** (01), 7–12.

Pender, G., Shevidchenko, A. B. & Chegini, A. 2007 Supplementary data confirming the relationship between critical Shields stress, grain size and bed slope. *Earth Surface Processes and Landforms* **32** (11), 1605–1610. DOI: 10.1002/esp.1588.

Phillips, B. C. & Sutherland, A. J. 1990 Temporal lag effect in bed load sediment transport. *Journal of Hydraulic Research* **28** (1), 5–23.

Piedra, M. M. 2010 *Flume Investigation of the Effects of sub-Threshold Rising Flows on the Entrainment of Gravel Beds*. Ph.D. thesis, University of Glasgow, Glasgow, UK.

Raven, E. K., Lane, S. N. & Bracken, L. J. 2010 Understanding sediment transfer and morphological change for managing upland gravel-bed rivers. *Progress in Physical Geography* **34** (1), 23–45.

Reid, I., Frostick, L. E. & Layman, J. T. 1985 The incidence and nature of bed load transport during flood flows in coarse-grained alluvial channels. *Earth Surface Processes and Landform* **10**, 33–44. doi:10.10023290100107.

Rodrigo-Comino, J., Keesstra, S. & Cerdà, A. 2018 Soil erosion as an environmental concern in vineyards: the case study of Celler del Roure, Eastern Spain, by means of rainfall simulation experiments. *Beverages* **4** (2), 31.

Rowinski, P. M. & Czernuszenko, W. 1998 Experimental study of river turbulence under unsteady conditions. *Acta Geophys* **46** (4), 461–480.

Seeger, M., Errea, M. P., Beguería, S., Arnáez, J., Martí, C. & García-Ruiz, J. M. 2004 Catchment soil moisture and rainfall characteristics as determinant factors for discharge/suspended sediment hysteretic loops in a small headwater catchment in the Spanish Pyrenees. *Journal of Hydrology* **288**, 299–311.

Shvidchenko, A. B. & Pender, G. 2000 Flume study of the effect of relative depth on the incipient motion of coarse uniform sediments. *Water Resources Research* **36** (2), 619–628.

Shvidchenko, A. B., Pender, G. & Hoey, T. B. 2001 Critical shear stress for incipient motion of sand/gravel streambed. *Water Resources Research* **37** (8), 2273–2283.

Soler, M., Latron, J. & Gallart, F. 2008 Relationships between suspended sediment concentrations and discharge in two small research basins in a mountainous Mediterranean area (Vallcebre, Eastern Pyrenees). *Geomorphology* **98** (1–2), 143–152.

Song, T. & Graf, W. H. 1997 Experimental study of bedload transport in unsteady open-channel flow. *International Journal of Sediment Research* **12** (3), 63–71.

Tsujimoto, T. 1989 Longitudinal stripes of alternate sorting due to cellular secondary currents. In: *Proceedings of the 23rd Congress of the International Association for Hydraulic Research*, Ottawa, Canada, Vol. 2, pp. 17–24.

Wang, Z. 1994 An experimental study of motion and deposition of gold particles in a mountain river. *Journal of Hydraulic Research* **32** (5), 643–648.

Wang, L. 2016 *Bedload Sediment Transport and bed Evolution in Steady and Unsteady Flows*. Ph.D dissertation, Heriot-Watt University, Edinburgh, UK, p. 334.

Wang, L., Cuthbertson, A. J. S., Pender, G. & Cao, Z. 2015 Experimental investigations of graded sediment transport under unsteady flow hydrographs. *International Journal of Sediment Research* **30** (4), 306–320.

Yen, C. L. & Lee, K. T. 1995 Bed topography and sediment sorting in channel bend with unsteady flow. *Journal of Hydraulic Engineering* **121** (8), 591–599.

Zabaleta, A., Martinez, M., Uriarte, J. A. & Antiguedad, I. 2007 Factors controlling suspended sediment yield during runoff events in small headwater catchments of the Basque Country. *Catena* **71**, 179–190.

First received 31 May 2019; accepted in revised form 6 August 2019. Available online 21 October 2019